

## EVOLUTION OF STRESSES And CURVATURES IN POROUS BODIES DURING COOLING

V. Cantavella<sup>(1)</sup>, A. Moreno<sup>(1)</sup>, A. Mezquita<sup>(1)</sup>, J.C. Jarque<sup>(1)</sup>,  
J. Barberá<sup>(2)</sup>, A. Palanques<sup>(2)</sup>

<sup>(1)</sup> Instituto de Tecnología Cerámica (ITC). Asociación de Investigación de las  
Industrias Cerámicas (AICE)  
Universitat Jaume I. Castellón. Spain.

<sup>(2)</sup> Cerámica Saloni, S.A. San Juan de Moró. Spain.

### ABSTRACT

*The rapid cooling of ceramic tiles in an industrial kiln produces temperature gradients inside the tiles. These gradients are known to cause residual stresses, following a process very similar to that of glass tempering.*

*In this study a method has been fine-tuned that allows the residual stresses to be measured in white wall tile bodies. The method has been used in pieces cooled rapidly under laboratory conditions, and the presence of residual stresses was verified.*

*In order to explain the residual stresses obtained under laboratory conditions, a thermo-mechanical model was developed that consisted of two parts: in the first (thermal) part, the temperature profiles inside the piece were calculated; in the second (mechanical) part, the dimensional stresses and the changes were obtained based on linear viscoelastic constitutive relations. The model was solved by a numerical method. The residual stress measurements made under laboratory conditions and the developed model allowed the parameters of the constitutive relations (variation of effective viscosity with temperature) to be determined.*

*Finally, tile surface temperature was measured during cooling in an industrial kiln, with the help of a temperature probe. This temperature value and the results obtained in the laboratory were used to estimate the evolution of curvature and stresses during and at the end of the cooling. The experimental measurement of the residual stresses led to a value very close to the one estimated with the model, confirming the model's applicability.*

## 1. INTRODUCTION

Cooling in industrial kilns takes place in three clearly differentiated steps: initial, indirect, and final cooling. The three take place at the highest possible speed compatible with the physical integrity of the tile; however, the high cooling rate causes a series of stresses to appear in the tile during cooling. If these stresses reach a critical value, tile failure will occur, leading to a defect known as *dunting*. Stresses below the critical value, though they may not lead to rupture, can generate microcracks that reduce mechanical strength significantly. Part of these stresses may remain inside the tiles after the firing. These stresses are called *residual stresses*.

Residual stresses can give rise to several problems:

1. If they relax, they lead to variations in curvature after firing. This is the phenomenon known as *delayed curvature*.
2. During cutting processes in tile installation, the tiles may break or be cut along non-desired paths.
3. During rectification the stressed areas are eliminated, as a result of which the rectification process is associated with a change in curvature.

There are basically two types of residual stresses in ceramic tiles: those originating from the fit between the glaze and the body<sup>[1]</sup> and those produced by the temperature gradients during cooling<sup>[2,3]</sup>. The latter have received much less attention than the former, partly because they are harder to study, and partly because they only begin to play a noteworthy role when factors appear such as the use of short industrial cycles, the manufacture of large-sized tiles, or tile polishing and rectification.

## 2. THEORETICAL MODEL

The calculation of the stresses that develop during cooling comprises a series of steps (figure 1). The first part of the calculation consists of solving the thermal problem. The starting point is knowing the geometry (thickness), thermal properties (thermal conductivity and specific heat), and density of the tile. With these properties, and knowledge of the tile surface temperature (or when this is unavailable, kiln temperature) and the heat transfer coefficients, and using the equations of heat transfer, it is possible to ascertain the temperature distribution inside the tile.

The second part of the calculation involves solving a mechanical problem. The temperature profile obtained previously and the constitutive relations, which establish the relation between stress and strain, serve as the starting point. The foregoing data, together with the equations of mechanical equilibrium, allow calculation of the displacements, i.e. the movements that the tile is going to undergo. Finally, the stresses that develop throughout the cooling are obtained.

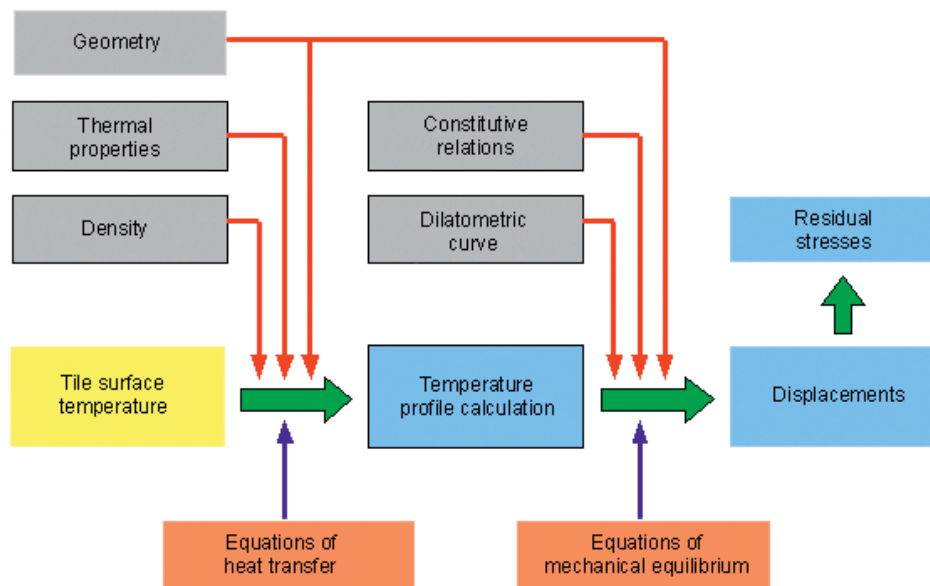


Figure 1. Steps for the calculation of residual stresses.

## 2.1. THERMAL CALCULATION

The equation of heat transmission in a non-steady state inside the tile adopts the form<sup>[4]</sup>:

$$\rho c_p \frac{\partial T}{\partial t} = k \nabla^2 T + G_E$$

Eq. 1

where:

T: temperature at a point in the tile at a given moment (°C)

t: time (s)

$\rho$ : density (kg/m<sup>3</sup>)

$c_p$ : specific heat (J/(kgK))

k: thermal conductivity (W/(mK))

$G_E$ : heat generation (W/m<sup>3</sup>)

The term heat generation corresponds to the heat absorbed or released by chemical reactions. During cooling all the important reactions from an energy viewpoint have already been completed; therefore, this term may be considered zero.

In order to solve the foregoing equation it is necessary to know the tile surface temperature, or the temperature in the kiln, and the heat transfer coefficients. Due to the difficulties of obtaining accurate values for these coefficients, it was decided to measure the tile surface temperature.

## 2.2. MECHANICAL CALCULATION

The constitutive relations establish the relation between the stress and the strain that a body undergoes. The simplest is Hooke's equation (linear elasticity); however, a law of this type is unable to explain the generation of residual stresses. One of the simplest constitutive relations that are able to explain the residual stresses are the linear viscoelastic constitutive relations, which may be written as:

$$\begin{aligned} \varepsilon_{e,x} &= \frac{1}{E} \sigma_x \\ \dot{\varepsilon}_{v,x} &= \frac{1}{3\eta} \sigma_x; \quad \eta = \eta_0 e^{\Theta/T} \end{aligned}$$

Eq. 2

where:

$\varepsilon_{e,x}$ : elastic strain along the x-axis

$\sigma_x$ : normal stress on a plane perpendicular to the x-axis (Pa)

E: modulus of elasticity (Pa)

$\eta$ : viscosity (Pa·s)

$\eta_0$ : pre-exponential factor (Pa·s)

$\Theta$ : constant (K)

With a view to simplifying the model, it was assumed that the modulus of elasticity was independent of temperature. This is simply an approximation, since it is known that there is a dependence of E on temperature; however, temperature may be expected to have a much smaller influence on E than on viscosity.

Finally, the equation of mechanical equilibrium may be written as<sup>[5]</sup>:

$$\begin{aligned} \sigma_{ij,j} + f_i &= 0 \\ \sigma_{ij} - \sigma_{ji} &= 0 \end{aligned}$$

Eq. 3

where  $\sigma_{ij}$  is the stress tensor and  $f_i$  the force per unit volume.

The finite element method was used to solve the previous equations, the tile being modelled as a bar (figure 2) divided into a series of cells (elements) with two nodes per element. Each node can move along the horizontal axis (U), vertical axis (W), or rotate ( $\Theta$ ). This reduces the problem to calculating the values of U, W, and  $\Theta$  in each node, along time.

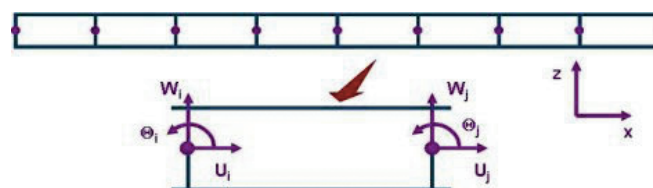


Figure 2. Finite element model used.

### 3. GENERATION OF STRESSES UNDER LABORATORY CONDITIONS

#### 3.1. DESCRIPTION OF THE ASSEMBLY

With a view to analysing the stresses that develop during cooling, 150x20 mm test pieces were pressed from a spray-dried powder. These test compacts were fired in an electric laboratory kiln at a temperature of 1130 °C and then rapidly cooled to ambient temperature (figure 3).

The cooling rate was regulated by modifying the distance between the test piece and refractory plates; the surface temperature of the test piece was measured with a K-type thermocouple connected to a data logging system.

The evolution of the temperature recorded as a function of time (series *T measured/rapid cooling* and *T measured/slow cooling*) is shown in figure 4. The thermocouple was initially cold and took a certain time to reach the test piece temperature. In order to calculate the *real* temperature of the test piece it was assumed that, initially, its temperature matched that of the kiln, and that the thermocouple behaved as a dynamic element that could be characterised by means of a first-order transfer function. These assumptions yielded the corrected curves shown in figure 4

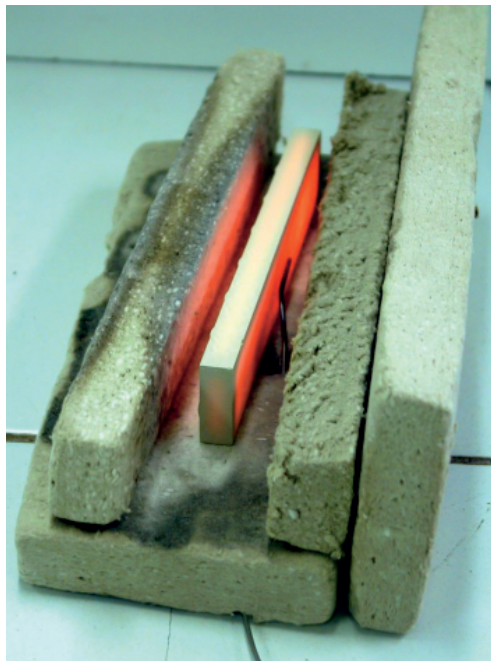


Figure 3. Assembly used to perform the rapid cooling.

#### 3.2. MEASUREMENT OF THE RESIDUAL STRESSES

##### 3.2.1. Description of the measurement method

The layer removal method was used to measure the residual stresses. The method consists of progressively reducing the thickness of the test piece by a mechanical method, and analysing the resulting dimensional change. The foundation of this

method, as well as the measured parameters: cumulative thickness of the removed layers ( $h_{c_i}$ ) and curvature ( $\kappa_i$ ), is shown in figure 5. The more stressed is the test piece, the greater will be the change in curvature that develops during machining.

Curvature can be calculated from the centre deflection ( $\delta_c$ ) from:

$$\kappa = \frac{8\delta_c}{L^2}$$

where L is the length of the test piece.

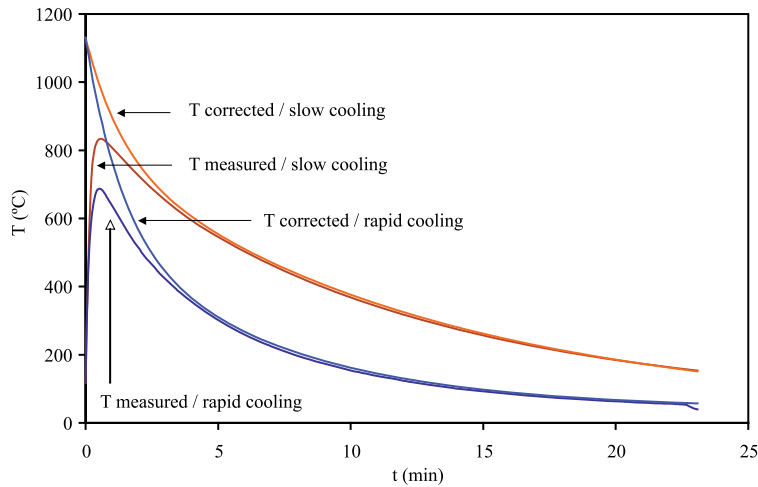


Figure 4. Evolution of test piece surface temperature with time

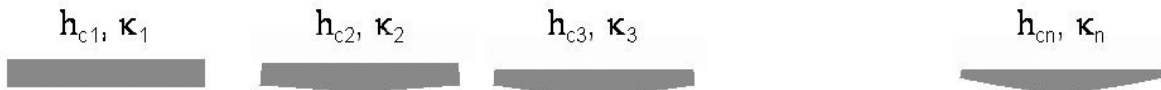


Figure 5. Foundation of the layer removal method. Measured parameters

In order to establish the relation between  $h_c$  and  $\kappa$ , and to evaluate the residual stresses, it is useful to use the free strain ( $\epsilon_f$ ) concept, which is the strain that a point in the piece would have if it were not subjected to any type of stresses (under conditions of very slow heating or cooling). Free strain, like the residual stresses, may vary throughout the thickness; i.e. it is a function of the position variable  $z$ , where  $z=0$  corresponds to the bottom surface and  $z=h_0$  to the top surface.

Instead of  $z$  it is more practical to define the dimensionless variable  $\zeta$  as:

$$\zeta = \frac{2z}{h_0} - 1$$

where  $h_0$  is the initial thickness of the test piece. The free strain may be written as a function of  $\zeta$ :  $\epsilon_f(\zeta)$ . In principle, the value of  $\epsilon_f(\zeta)$  is unknown. It is quite usual to

decompose  $\varepsilon_f(\zeta)$  as a linear combination of certain *basis functions*  $\phi_k(\zeta)$  defined in the range  $[-1,1]$ . In the calculations performed, Legendre polynomials  $P_k(\zeta)$  were used as basis functions:

$$\varepsilon_f(\zeta) = \sum_{k=0}^{\infty} \lambda_k \phi_k(\zeta) = \sum_{k=0}^{\infty} \lambda_k P_k(\zeta)$$

Eq. 4

Where the Legendre polynomials are defined by the Rodrigues equation<sup>[6]</sup>:

$$P_k(x) = \frac{1}{2^k k!} \frac{d^k}{dx^k} (x^2 - 1)^k$$

Eq. 5

The first five Legendre polynomials are shown in figure 6.

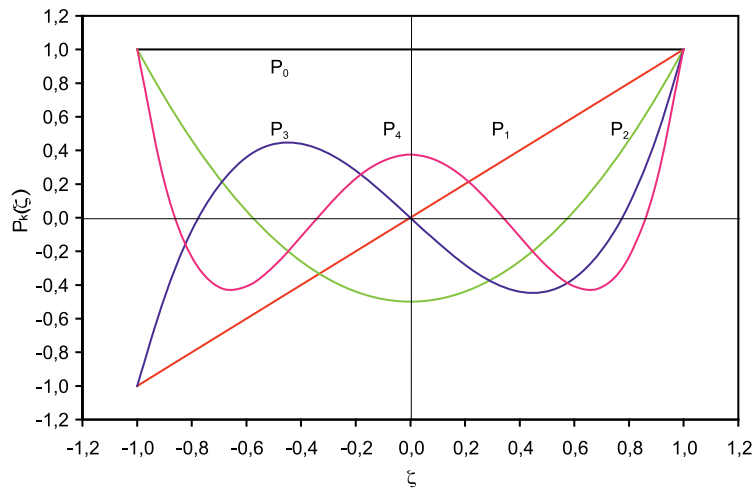


Figure 6. Graphic representation of the first five Legendre polynomials.

The advantage of using these polynomials is that the terms  $k=0$  and  $k=1$  lead to dimensional changes in the piece, but not to residual stresses. It was further verified experimentally that the terms corresponding to  $k \geq 3$  played no significant role. Under these conditions, eq. 4 becomes:

$$\varepsilon_f(\zeta) = \lambda_2 P_2(\zeta)$$

Eq. 6

The foregoing equation and the elasticity equations allow the relation to be calculated between the cumulative thickness of the removed layers,  $h_c$  and the variation in curvature that the piece undergoes.

$$h_0 \Delta \kappa = -6 \lambda_2 \frac{\Delta h_c}{h_0} \rightarrow \Delta \kappa' = -6 \lambda_2 h_c'$$

Eq. 7

where  $\Delta\kappa'$  is the variation of the dimensionless curvature and  $h_c'$  is the dimensionless thickness of the removed layers. Finally, the stress profile is given by the expression:

$$\sigma_r(\zeta) = -E\lambda_2 P_2(\zeta)$$

Eq. 8

where  $\sigma_r(\zeta)$  is the residual stress and E the modulus of elasticity. According to eq. 8, under the conditions indicated previously, the stress profile is parabolic. The highest stress values are found at the surface, where  $\zeta=\pm 1$ ,  $P_2(\pm 1)=1$ , the value of these stresses being  $\sigma_{res}=-E\lambda_2$ . Therefore,  $\lambda_2$  is a direct measure of the value of the residual stresses.

### 3.2.2. Results of the residual stress measurement

The evolution of curvature as a function of the removed dimensionless thickness is plotted in figure 7. It shows that the points obtained fit a straight line, as predicted by eq. 7. In addition, as the cooling becomes faster, the slope becomes steeper.

The foregoing data allowed figure 8 to be obtained, in which the stress profile throughout the thickness of the piece has been plotted. It shows that a negative stress (compression) develops near the surface and a positive stress (tension) near the centre. This corresponds to the typical stress profile obtained during tempering of a material like glass.

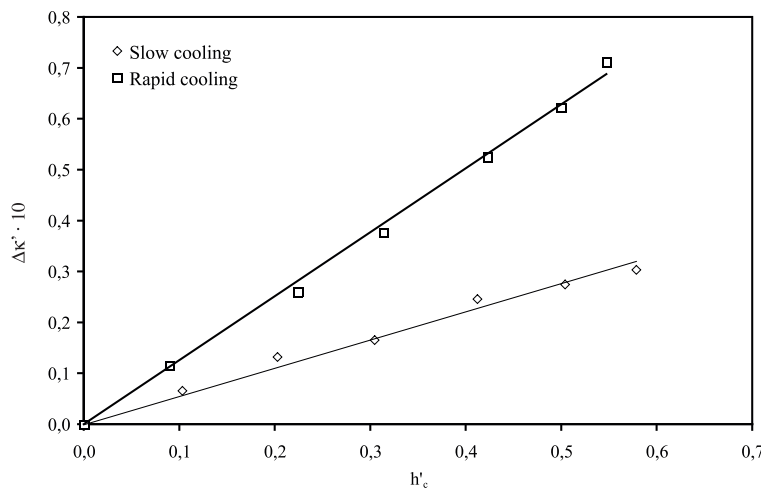


Figure 7. Variation of curvature as a function of cumulative removed layer thickness.

### 3.3. APPLICATION OF THE MODEL TO THE LABORATORY TESTS

The surface temperature curves of the piece (figure 4) and the values of the thermal properties were used to determine the temperature profile inside the piece.

In order to solve the mechanical problem it was necessary to determine the parameters of eq. 2. The modulus of elasticity was measured using the three-point bending test. The determination of parameters  $\eta_0$  and  $\Theta$  was more complex, so that

it was decided to leave them as fitting parameters, determining their value from the experimental results of the residual stresses (figure 8).

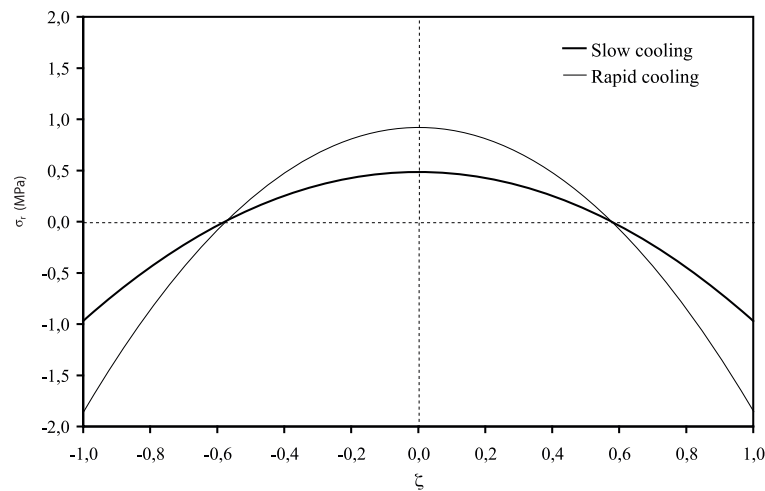


Figure 8. Stress profile inside the test piece, for the two analysed cooling rates.

The results of the application of the model are given in figure 9 for slow cooling and in figure 10 for fast cooling. The evolution of temperature during cooling and the stress inside the pieces have been plotted in both graphs.

The stress inside the piece varies throughout the direction of the thickness, as indicated previously. This profile can also be expressed as a linear combination of Legendre polynomials, in an analogous form to eq. 4, yielding:

$$\sigma_r(\zeta) = -E \sum_{k=2}^{\infty} \lambda'_k P_k(\zeta)$$

Eq. 9

If the temperature in the piece is uniform, the parameters  $\lambda'_k$  of the previous equation coincide with  $\lambda_k$  of eq. 4. One of the uses of eq. 9 is that it allows the stress profile  $\sigma_r(\zeta, t)$  to be expressed, which depends on the coordinate of thickness and time, as a set of functions  $\lambda'_k(t)$  that only depend on time, not on  $\zeta$ . Instead of using  $\lambda'_k E$  it is possible to work with the product  $\lambda'_k E$ , which has stress dimensions and is therefore more directly related to the stress profile.

It may be observed in figure 9 that  $\lambda'_2 E$  (Pol-2 series) is the most important component of the stress profile. A maximum appears at the beginning, owing to the initial rapid cooling. At about 5 minutes there is a second maximum, even though the cooling rate continues to decrease. This second maximum occurs at about 573 °C, and is due to the allotropic transformation of quartz. Once the transition region has been crossed, the value of  $\lambda'_2 E$  decreases; however, at the end of the cooling, it is not zero. The remaining value is the residual stress.

The term  $\lambda'_3 E$  is constant and equal to zero, because the cooling is symmetrical and, hence, so is the stress profile. In fact, all  $\lambda'_k E$  terms with an odd  $k$  must be zero.

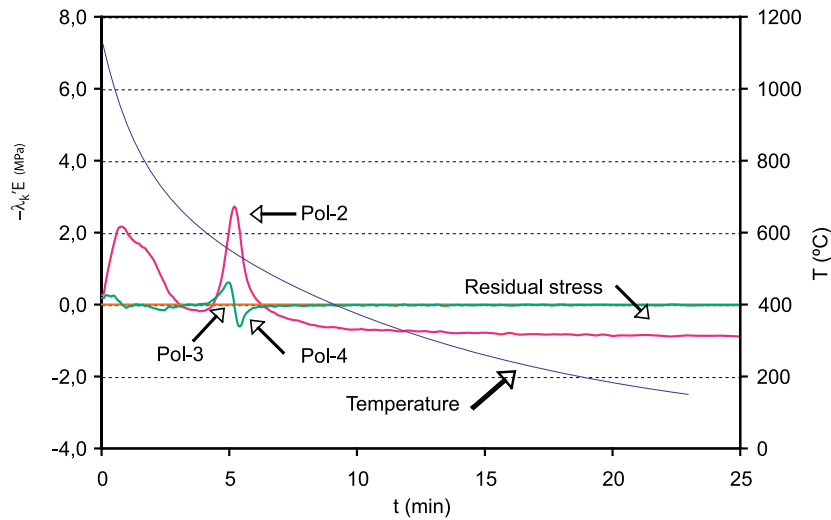


Figure 9. Evolution of the coefficients of the Legendre polynomials  $P_2$ ,  $P_3$ , and  $P_4$ . Slow cooling.

Finally, the term  $\lambda_4 E$  (and those of higher order) are smaller, and have a certain importance solely near the quartz transition area. Once the cooling has ended, only  $\lambda_2 E$   $t$  persists, which explains why the experimentally measured profile is parabolic.

When the cooling is performed at a faster rate, similar curves are obtained (figure 10), but the value of all stresses is quantitatively greater. In particular, it is observed that the stress during the quartz transition is very high. If this stress exceeds the mechanical strength, *dunting* (rupture of the piece) can occur.

It is also noted that, when the cooling rate increases, the final residual stress profile continues to be parabolic, though with a greater stress value.

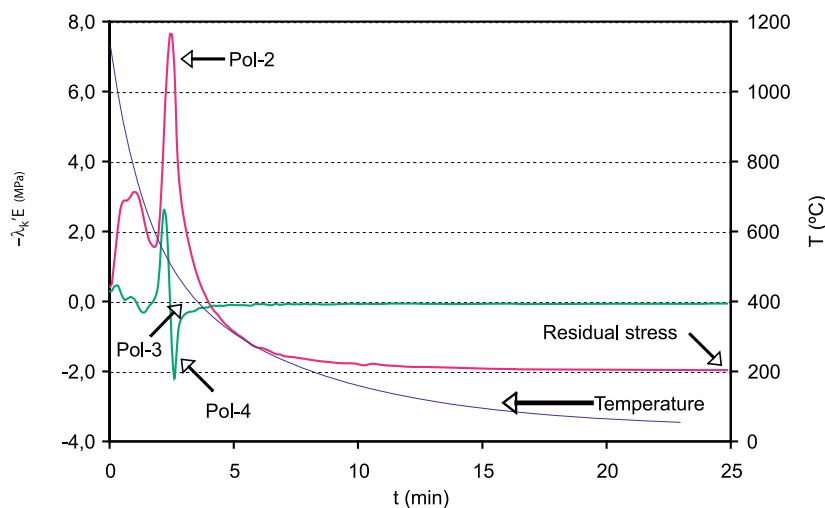


Figure 10. Evolution of the coefficients of the Legendre polynomials  $P_2$ ,  $P_3$ , and  $P_4$ . Rapid cooling.

The foregoing calculations allowed estimation of the parameters of the constitutive relations (eq. 2), which yielded:

$$\eta_0 = 1.96 \cdot 10^{11} \text{ Pa}\cdot\text{s}$$

$$\Theta = 2200 \text{ K}$$

## 4. INDUSTRIAL APPLICATION

### 4.1. THERMAL CALCULATION

In order to calculate the stresses and the evolution of curvature in the tiles under industrial conditions, the procedure indicated in figure 1 was followed. A kiln was selected in which white-body wall tiles, size 600x300 mm, were being processed.

The first step was to measure the temperature at the top and bottom tile surfaces<sup>[7]</sup>, for which a *Datapaq* temperature probe was used. The evolution of tile surface temperature, as well as that of the thermocouples in the kiln, is plotted in figure 11.

It is observed that there may be significant differences between the temperatures recorded by the kiln thermocouples and the temperatures at the tile surface.

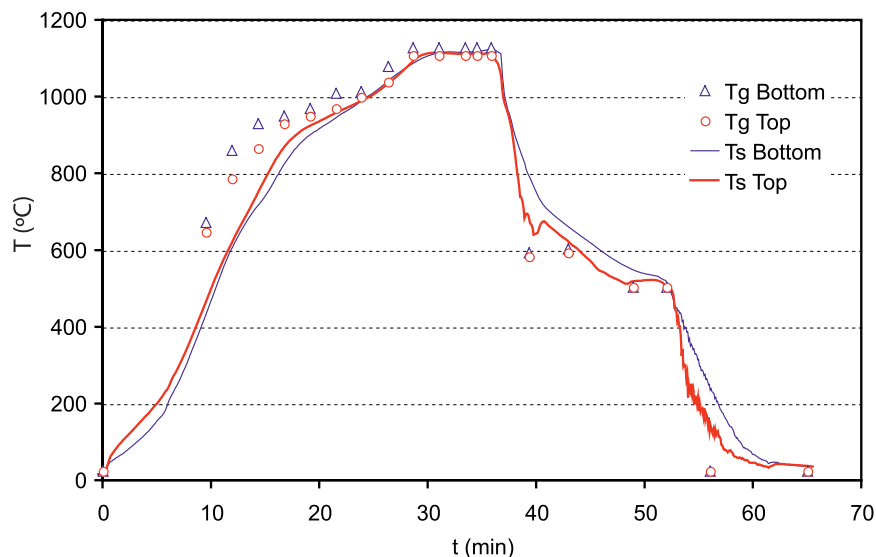


Figure 11. Kiln gas temperature ( $T_g$ ; circles and triangles) and tile surface temperature ( $T_s$ ; solid lines)

### 4.2. EVOLUTION OF TILE CURVATURE

The temperature at the top and bottom tile surfaces, as well as tile curvature, is plotted in figure 12. At the beginning, during the initial rapid cooling, the tile exhibits a negative deflection (concave curvature), because the top surface temperature is lower, which causes this surface to shrink more.

Another maximum appears in the quartz firing range. In this case, the curvature exceeds -4.5 mm, and is caused by the high coefficient of thermal expansion in this stretch.

In the final cooling, the temperature difference is significant, and produces a new curvature maximum. At the kiln exit the tile is once again flat.

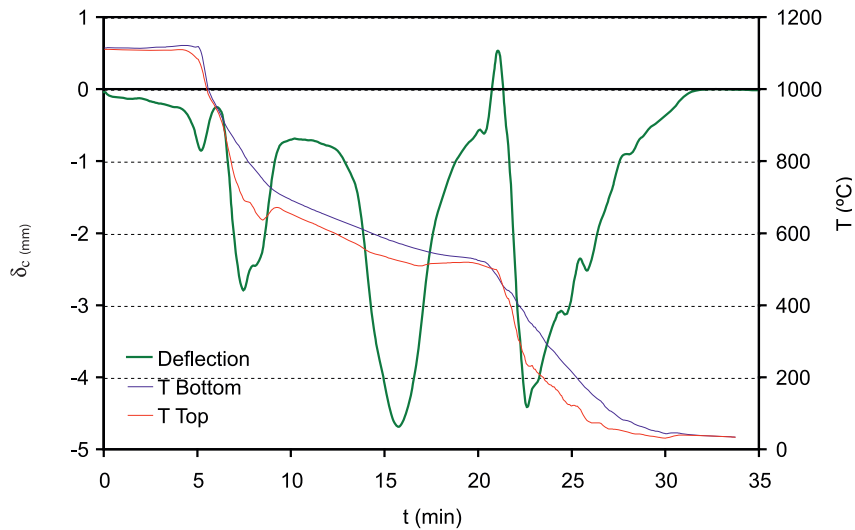


Figure 12. Calculation of the evolution of the curvature deflection of a tile body during industrial cooling.

The evolution of curvature during cooling is, therefore, very complex. It may be noted, furthermore, that in the calculations performed the glaze/body fit has not been taken into account, nor has the existence of possible *predeformations* generated during heating.

#### 4.3. CALCULATION OF RESIDUAL STRESSES

The stress distribution inside the tile and throughout the kiln has been plotted in figure 13. The t-axis represents the time that elapses after the tile has left the firing area, and  $\zeta$  is the dimensionless position inside the tile. The values of  $\zeta$  in the foreground plane correspond to the stresses at the bottom surface, while those in the background plane correspond to the stresses at the top surface.

There are three periods in tile cooling in which stresses are large: cooling start, the quartz transition area, and the beginning of the final cooling. These areas match those in which significant curvature changes occur.

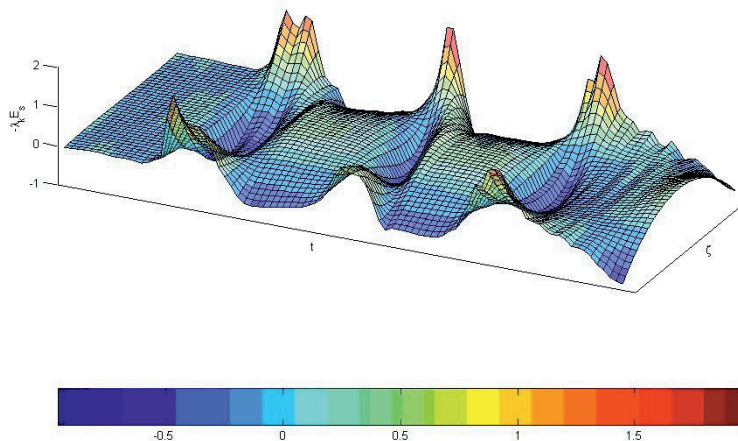


Figure 13. Calculation of the evolution of the curvature deflection in the tile body during industrial cooling.

As soon as the tile leaves the peak temperature area, tensile stresses appear at the surfaces and compression stresses in the centre. These stresses decrease and even reverse after 10 minutes. Entry into the quartz transition area causes important stresses to appear again, which continue to be tensile stresses at the surface and compression stresses in the centre. In addition, the stress in the tile top surface is higher because the cooling is abrupt through this surface. It is interesting to note that the maximum stress peak is located exactly in the indirect cooling zone, which means that the curve design is appropriate. It also indicates that the extent of the indirect cooling zone is excessively large; possibly owing to the oversizing factor used by the kiln manufacturer.

In the final indirect cooling zone the  $\beta$ -quartz  $\rightarrow$   $\alpha$ -quartz transition has already occurred, and the stresses reverse again.

When the final cooling is reached, the surfaces are again subject to tension so that they shrink. This stress decreases progressively as the thermal difference between the surface and the centre decreases. When the tile leaves the kiln it exhibits residual stresses that are compression stresses at the surface and tensile stresses in the centre.

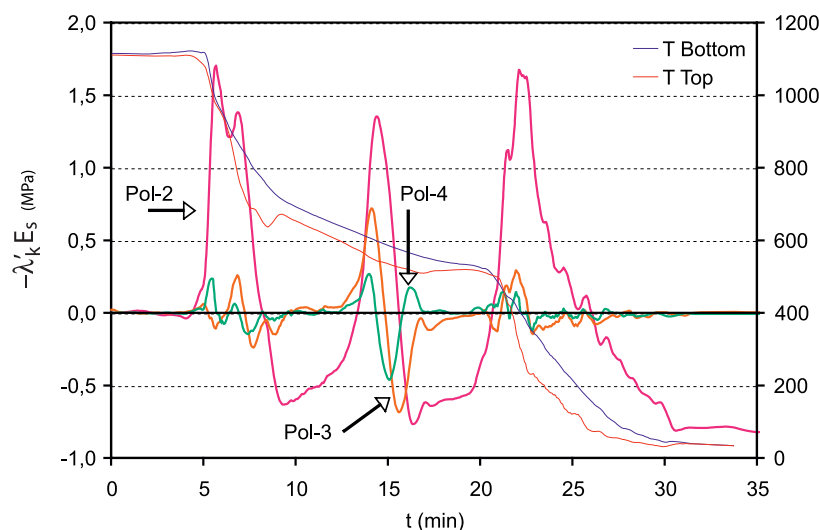


Figure 14. Evolution of the coefficients of the Legendre polynomials  $P_2$ ,  $P_3$ , and  $P_4$ . Industrial cooling.

The evolution of the coefficients of the Legendre polynomials  $\lambda_2$ ,  $\lambda_3$ , and  $\lambda_4$  is shown in figure 14. The main difference between figure 14 and the one obtained in the laboratory is its greater complexity.  $\lambda_3$  becomes important, especially in the quartz transition area. This is a very clear indication that the cooling is not uniform (cooling is greater through the top than through the bottom). Despite the complexity of stress evolution during cooling, the tile displays a relatively simple profile at the kiln exit: only  $\lambda'_2$  differs from zero.

The stress profile inside the piece, calculated theoretically with the developed model, is shown in a solid line in figure 15. The points correspond to the profile

determined experimentally in a tile fired under industrial conditions. Good agreement is observed, which validates the model for the estimation of the stresses generated under industrial conditions.

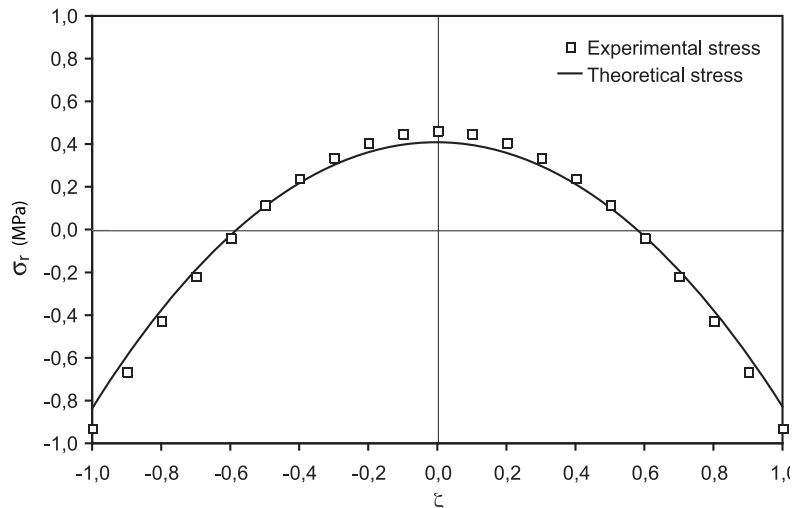


Figure 15. Comparison of the theoretical residual stress profile and the one calculated experimentally from the developed model.

## 5. CONCLUSIONS

- A procedure has been developed that allows the residual stresses inside ceramic tiles to be measured.
- During the industrial cooling of porous wall tiles, residual stresses develop as a result of thermal gradients in the tiles. This phenomenon can be reproduced on a laboratory scale, withdrawing the tile from the kiln at peak temperature to force rapid cooling.
- The residual stress profile, in both industrial tiles and test pieces in the laboratory, is basically parabolic, with tensile stress at the surface and compression stress in the middle.
- A model has been developed that allows the residual stresses and the evolution of tile curvature during cooling in the kiln to be calculated. The model is based on data obtained in laboratory tests and on the measurement of tile surface temperature under industrial conditions.
- The measurement of the residual stresses of industrially fired tiles matches the theoretically calculated values.
- The developed model predicts that the tile will have a concave curvature during most of the cooling. This curvature displays three maximum values, which coincide with cooling start, the quartz transition area, and the beginning of final cooling.

## REFERENCES

- [1] AMORÓS, J.L. et al. Acuerdo esmalte-soporte (I). Causas y factores de los que depende. *Téc. Cerám.*, **179**, 644-657, 1989.
- [2] NONI, A. de et al. Influencia del enfriamiento de la etapa de cocción sobre las propiedades mecánicas del gres porcelánico. *Bol. Soc. Esp. Ceram. Vidr.* **46 (4)**, 163-170, 2007.
- [3] CANTAVELLA, V. et al. Residual stresses in ceramics. *2006 FGM Multiscale & Functionally Graded Materials Conference*. Ko Olina - Hawaii, 15<sup>th</sup>-18<sup>th</sup> October 2006.
- [4] INCROPERA, F.P.; WITT, D.P. de. *Fundamentals of heat and mass transfer*. Singapore: John Wiley & Sons, 1990.
- [5] SAMARTÍN QUIROGA, A. *Curso de elasticidad*. Madrid: Bellisco, 1990.
- [6] BRONSHTEIN, I.; SEMENDIAEV, K. *Manual de matemáticas para ingenieros y estudiantes*. Madrid: Rubiños, 1993.
- [7] CANTAVELLA, V. et al. Temperature distribution inside a ceramic tile during industrial firing. In the *IX World Congress on Ceramic Tile Quality - Qualicer 2006*. Castellón: Cámara Oficial de Comercio, Industria y Navegación, 2006. pp. P.BC147-P.BC160, 2006.